

Particle flow calorimetry

This article has been downloaded from IOPscience. Please scroll down to see the full text article.

2008 J. Phys.: Conf. Ser. 110 092032

(<http://iopscience.iop.org/1742-6596/110/9/092032>)

View [the table of contents for this issue](#), or go to the [journal homepage](#) for more

Download details:

IP Address: 38.107.179.210

The article was downloaded on 15/02/2012 at 01:38

Please note that [terms and conditions apply](#).

Particle Flow Calorimetry

Mark Thomson

University of Cambridge, Cavendish Laboratory, JJ Thomson Avenue, CB3 0HE, UK

E-mail: mark.thomson@hep.phy.cam.ac.uk

Abstract. One of the most important requirements for a detector at the ILC is good jet energy resolution. It is widely believed that the particle flow approach to calorimetry is the key to achieving the ILC goal of a di-jet invariant mass resolution $\sigma_m/m < \Gamma_Z/m_Z$. This paper describes the current performance of the PANDORAPFA particle flow algorithm. For simulated light quark jets it is shown that a jet energy resolution of better than $\sigma_E/E \approx 3.4\%$ can be achieved for jet energies in the range 45 – 250 GeV.

1. Introduction

Many of the interesting physics processes at the ILC will be characterised by multi-jet final states, often accompanied by charged leptons and/or missing transverse energy associated with neutrinos or the lightest super-symmetric particles. The reconstruction of the invariant masses of two or more jets will provide a powerful tool for event reconstruction and identification. Unlike at LEP, where kinematic fitting[1] enabled precise jet-jet invariant mass reconstruction almost independent of the jet energy resolution, at the ILC this mass reconstruction will rely on the detector having excellent jet energy resolution. The ILC goal is to achieve a mass resolution for $W \rightarrow q\bar{q}$ and $Z \rightarrow q\bar{q}$ decays which is comparable to their natural widths, i.e. $\sigma_m/m = 2.7\% \approx \Gamma_W/m_W \approx \Gamma_Z/m_Z$. For a traditional calorimetric approach, a jet energy resolution of $\sigma_E/E = \alpha/\sqrt{E(\text{GeV})}$ leads to a di-jet mass resolution of roughly $\sigma_m/m = \alpha/\sqrt{E_{jj}(\text{GeV})}$, where E_{jj} is the energy of the di-jet system. At the ILC typical di-jet energies will be in the range 150 – 350 GeV, suggesting the goal of $\sigma_E/E \sim 0.3/\sqrt{E(\text{GeV})}$. This is more than a factor two better than the best jet energy resolution achieved at LEP, $\sigma_E/E = 0.6(1 + |\cos \theta|)/\sqrt{E(\text{GeV})}$ [2].

2. The Particle Flow Approach to Calorimetry

It is widely believed that the most promising strategy for achieving the ILC jet energy goal is the particle flow analysis (PFA) approach to calorimetry. PFA requires the reconstruction of the four-vectors of all visible particles in an event. The reconstructed jet energy is the sum of the energies of the individual particles. In PFA the momenta of charged particles are measured in the tracking detectors, while the energy measurements for photons and neutral hadrons are obtained from the calorimeters. The crucial step in PFA is to assign the correct calorimeter hits to reconstructed particles, requiring efficient separation of nearby showers.

Measurements of jet fragmentation at LEP have provided detailed information on the particle composition of jets (e.g. [3, 4]). On average, after the decay of short-lived particles, roughly 62% of the energy of jets is carried by charged particles (mainly hadrons), around 27% by photons,

about 10% by long-lived neutral hadrons (*e.g.* n/K_L^0), and around 1.5% by neutrinos. Assuming calorimeter resolutions of $\sigma_E/E = 0.15/\sqrt{E(\text{GeV})}$ for photons and $\sigma_E/E = 0.55\sqrt{E(\text{GeV})}$ for hadrons, a jet energy resolution of $0.19/\sqrt{E(\text{GeV})}$ is obtained. In practise it is not possible to reach this level of performance for two main reasons. Firstly, particles travelling at small angles to the beam axis will not be detected. Secondly, and more importantly, it is not possible to perfectly associate all energy deposits with the correct particles. For example, if a photon is not resolved from a charged hadron shower, the photon energy is not counted. Similarly, if part of charged hadron shower is identified as a separate cluster the energy is effectively double-counted. This *confusion* degrades particle flow performance. Because confusion, rather than calorimetric performance, determines the overall performance, the jet energy resolution achieved will not, in general, be of the form $\sigma_E/E = \alpha/\sqrt{E(\text{GeV})}$.

The crucial aspect of particle flow is the ability to correctly assign calorimeter energy deposits to the correct reconstructed particles. This places stringent requirements on the granularity of electromagnetic and hadron calorimeters. Consequently, particle flow performance is one of the main factors driving the overall ILC detector design. It should be noted that the jet energy resolution obtained for a particular detector concept is the combination of the intrinsic detector performance and the performance of the PFA software.

3. The PandoraPFA Particle Flow Algorithm

PANDORAPFA is a C++ implementation of a PFA algorithm running in the MARLIN[5, 6] framework. It was designed to be sufficiently generic for ILC detector optimisation studies and was developed and optimised using events generated with the MOKKA[7] program, which provides a GEANT4[8] simulation of the Tesla TDR[9] detector concept. The PANDORAPFA algorithm[10] performs both calorimeter clustering and particle flow in eight main stages: **i) Tracking:** the track *pattern recognition* is performed using Monte Carlo information[5] but the track parameters and $kink/V^0$ are obtained from simple helical fits. **ii) Calorimeter Hit Selection and Ordering:** isolated hits, defined on the basis of proximity to other hits, are removed from the initial clustering stage. The remaining hits are ordered into *pseudo-layers* which follow the detector geometry so that particles propagating outward from the interaction region will cross successive pseudo-layers. **iii) Clustering:** the main clustering algorithm is a cone-based forward projective method[10] working from innermost to outermost pseudo-layer. The algorithm starts by *seeding* clusters using the projections of reconstructed tracks onto the front face of the calorimeter. **iv) Topological Cluster Merging:** by design the initial clustering errs on the side of splitting up true clusters rather than clustering energy deposits from more than one particle. Clusters are combined on the basis of clear topological signatures, *e.g.* looping minimum ionising calorimeter tracks, back-scattered tracks and showers associated with a hadronic interaction. The cluster merging algorithms are only applied to clusters which have not been identified as photons. **v) Statistical Re-clustering:** The previous four stages of the algorithm were found to perform well for jets with energy less than ~ 50 GeV. However, at higher energies the performance degrades rapidly due to the increasing overlap between hadronic showers from different particles. If the track momentum is incompatible with the energy of the associated cluster, $E_{\text{CLUSTER}} - E_{\text{TRACK}} > 3.5\sigma_E$, re-clustering is performed by applying the clustering algorithm above, with different parameters, until the cluster splits to give an acceptable track-cluster energy match. **vi) Photon Recovery and Identification:** A more sophisticated, shower-profile based, photon-identification algorithm is then applied to the clusters, improving the tagging of photons and recovery of primary photons merged with hadronic showers. **vii) Fragment Removal:** At this stage there is still a significant number of “neutral clusters” which are *fragments* of charged particle hadronic showers. These clusters are identified based on a number of variables and the change in track-cluster matching χ^2 that would be obtained if the cluster in questions is merged with an existing cluster which is matched to a track. **viii)**

Formation of Particle Flow Objects: The final stage of the algorithm is to create Particle Flow Objects (PFOs) from the results of the clustering.

4. Current Performance

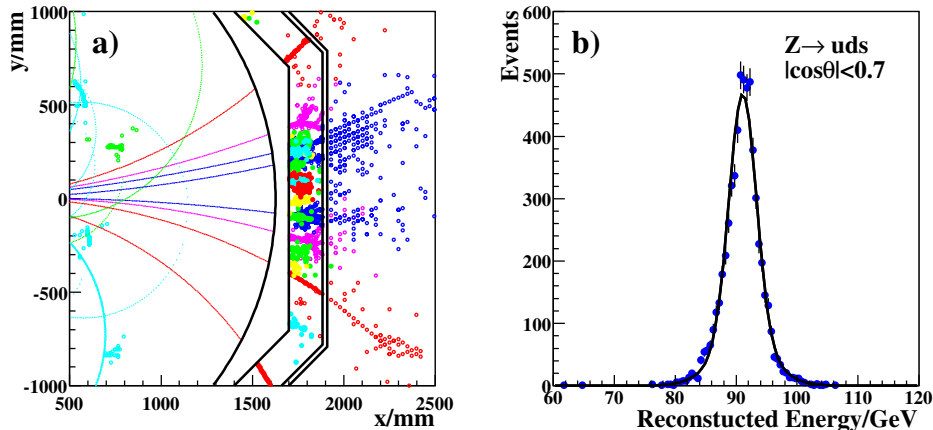


Figure 1. a) PANDORAPFA reconstruction of a 100 GeV jet in the MOKKA simulation of the Tesla TDR detector. b) The total reconstructed energy from reconstructed PFOs in $Z \rightarrow uds$ events for initial quark directions within the polar angle acceptance $|\cos\theta_{q\bar{q}}| < 0.7$. The solid line shows a fit to two Gaussians with a common mean; the broader Gaussian is constrained to contain 25% of the events. The narrow Gaussian has a width of 2.2 GeV.

Figure 1a) shows an example of a PANDORAPFA reconstruction of a 100 GeV jet from a $Z \rightarrow u\bar{u}$ decay at $\sqrt{s} = 200$ GeV. The ability to track particles in the high granularity Tesla TDR calorimeter can be seen clearly. Figure 1b) shows the total PFA reconstructed energy for $Z \rightarrow uds$ events with $|\cos\theta_{q\bar{q}}| < 0.7$, where $\theta_{q\bar{q}}$ is the polar angle of the generated $q\bar{q}$ system. These events were generated at $\sqrt{s} = 91.2$ GeV using the Tesla TDR detector model with a HCAL consisting of 63 layers and in total 6.9 interaction lengths. The root-mean-square deviation from the mean (rms) of the distribution is 2.8 GeV. However, quoting the rms as a measure of the performance over-emphasises the importance of the tails. It is conventional to quote the performance in terms of rms_{90} , which is defined as the rms in the smallest range of reconstructed energy which contains 90% of the events. For the data shown in figure 1b) the resolution achieved is $\text{rms}_{90}/E = 0.23/\sqrt{E(\text{GeV})}$, equivalent to a single jet energy resolution of 3.3%. Figure 2 shows the jet energy resolution for $Z \rightarrow uds$ events plotted against $|\cos\theta_{q\bar{q}}|$ for four different values of \sqrt{s} . The current performance is summarised in table 1. The observed jet energy resolution in simulated events is not described by the expression $\sigma_E/E = \alpha/\sqrt{E(\text{GeV})}$. This is not surprising, as the particle density increases it becomes harder to correctly associate the calorimetric energy deposits to the particles and the confusion term increases. The table also shows a measure of the single jet energy resolution, obtained by dividing rms_{90} by $\sqrt{2}$. For the jet energies considered (45 – 250 GeV) the fractional energy resolution is significantly better than the ILC requirement of 3.8% obtained from the consideration of gauge boson di-jet mass resolution. It should be noted that in a real physics analysis the performance is likely to be degraded by jet finding, jet-pairing and the presence of missing energy from semi-leptonic heavy quark decays. Nevertheless the results presented in this paper already provide a strong indication that Particle Flow Calorimetry will be able to deliver the ILC jet energy goals and it is expected that the performance of PANDORAPFA will improve with future refinements to the algorithm.

5. Conclusions

Particle flow calorimetry is widely believed to be the key to reaching the ILC jet energy resolution goal of a di-boson mass resolution of $\sigma_m/m < 2.7\%$. Consequently, the design and optimisation of detectors for the ILC depends both on hardware and on sophisticated software reconstruction. Based on the PANDORAPFA reconstruction of simulated events in Tesla TDR detector concept, it has now been demonstrated that particle flow calorimetry can meet this goal at the ILC.

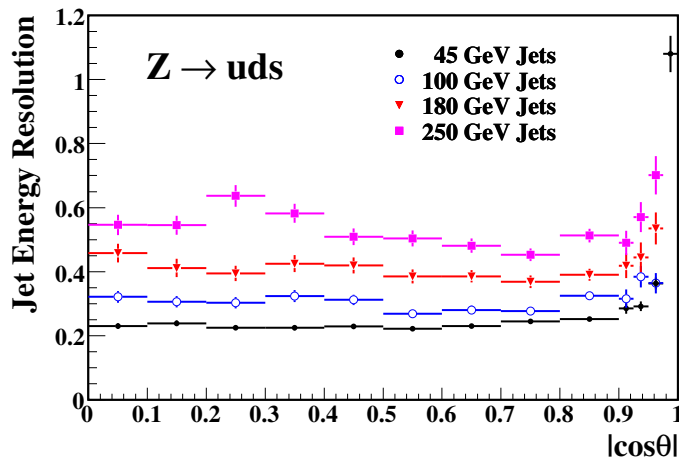


Figure 2. The jet energy resolution, defined as the α in $\sigma_E/E = \alpha\sqrt{E(\text{GeV})}$, plotted versus $\cos\theta_{q\bar{q}}$ for four different values of \sqrt{s} .

Table 1. Jet energy resolution for $Z \rightarrow uds$ events with $|\cos\theta_{q\bar{q}}| < 0.7$, expressed as, rms_{90} for the di-jet energy distribution, the effective constant α in $\text{rms}_{90}/E = \alpha(E_{jj})/\sqrt{E_{jj}(\text{GeV})}$, and the fractional jet energy resolution for a single jet.

Jet Energy	rms_{90}	$\text{rms}_{90}/\sqrt{E_{jj}(\text{GeV})}$	$\text{rms}_{90}/\sqrt{2}E_j$
45 GeV	2.2 GeV	23 %	3.3 %
100 GeV	4.1 GeV	29 %	2.9 %
180 GeV	7.4 GeV	39 %	2.9 %
250 GeV	12.0 GeV	54 %	3.4 %

- [1] M. A. Thomson, Proc. of EPS-HEP 2003, Aachen. Topical Vol. of *Eur. Phys. J. C Direct* (2004).
- [2] ALEPH Collaboration, D. Buskulic et al., *Nucl. Inst. Meth.* **A360** (1995) 481.
- [3] I.G. Knowles and G.D. Lafferty, *J. Phys.* **G23** (1997) 731.
- [4] M. G. Green, S. L. Lloyd, P. N. Ratoff and D. R. Ward, "Electron-Positron Physics at the Z", IoP Publishing (1998).
- [5] <http://www-flc.desy.de/ilcsoft/ilcsoftware/>.
- [6] F. Gaede, "Status of ILC-LDC Core Software", Proceedings of LCWS07, DESY, June 2007.
- [7] <http://polywww.in2p3.fr/activites/physique/geant4/tesla/www/mokka/>.
- [8] GEANT4 collaboration, S. Agostinelli et al., *Nucl. Instr. and Meth.* **A506** (2003) 3;
 GEANT4 collaboration, J. Allison et al., *IEEE Trans. Nucl. Sci.* 53 (2006) 1.
- [9] TESLA Technical Design Report, DESY 2001-011, ECFA 2001-2009 (2001).
- [10] M. A. Thomson, Proc. of LCWS07, DESY, June 2007, arXiv:physics/0709.1360.